X-ray Microbeam Strain Measurements in Polycrystalline Films

G.S. Cargill,[1] L.E. Moyer,[1] B.C. Larson,[2] W. Yang,[2] G.E. Ice[2]
[1]Department of Materials Science and Engineering, Lehigh University, Bethlehem, PA, U.S.A.
[2]Solid State Division, Oak Ridge National Laboratory (ORNL), Oak Ridge, TN, U.S.A.

Introduction

Integrated circuit (IC) devices are typically connected by patterned lines of a passivated polycrystalline metal, usually copper or aluminum. As IC devices and interconnects continue to decrease in size, electrical performance and mechanical reliability become greater concerns. Thermal strains develop in interconnects during fabrication and during operation at elevated temperatures because of the difference in the coefficient of thermal expansion between interconnects and surrounding layers. These strains can lead to failures from voids and hillocks in interconnects. X-ray diffraction is a well-established technique for measuring average elastic strains in polycrystalline materials. Recent advances in third-generation synchrotron sources and focusing optics now provide the means for grain-by-grain x-ray measurements [1-3]. We have carried out x-ray microbeam strain measurements in polycrystalline Cu and Al films [4, 5].

Methods and Materials

Kirkpatrick-Baez mirrors are used to obtain a submicron x-ray beam for microdiffraction. The sample is positioned on a translation stage at an angle of 45° from the incoming beam. A charge-coupled device (CCD) detector located directly above the sample records the Laue diffraction pattern.

A computer program developed at ORNL [1] calculates the orientation matrix of each grain in the Laue pattern. The program also measures the deviations of the Laue spots from the unstrained positions to obtain a complete deviatoric strain tensor.

A 1-_m-thick polycrystalline Cu film with a (111) fiber texture on a (001)-oriented single-crystal Si substrate was investigated. The sample was heated to 400°C, held for 1 h, and then cooled to room temperature. Microdiffraction measurements were made at room temperature after the thermal cycle. Both white x-ray area scans and monochromatic energy scans were performed.

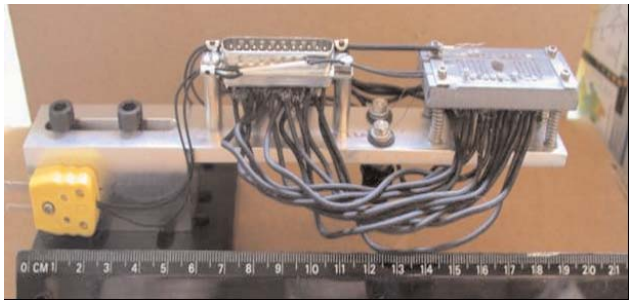

FIG. 1. Heating stage for in-situ microdiffraction experiments.

Another sample investigated was a 2-_m-thick polycrystalline Al film with a (111) fiber texture on a glass substrate. A heating stage, shown in Fig. 1, was used to heat the sample to 300°C for in situ x-ray microdiffraction measurements during thermal cycling.

Results

X-ray microbeam diffraction measurements at room temperature were made within days after the heat treatment for the Cu sample. Similar experiments were reported by Chung et al. [2] and Tamura et al. [3]. The crystallographic orientation and the deviatoric strain tensor ε_{ij}* were determined for each grain. The average grain size for this sample was approximately 1 _m, although some grains were larger. A grain orientation map for this sample is shown in Fig. 2. Each of the small squares in Fig. 2 is 0.5 × 0.5 _m, and the entire mapped area is 2.5 × 7.5 _m. Boundaries within individual squares were drawn to indicate which grains

FIG. 2. Grain orientation map for 1-_m-thick Cu sample.

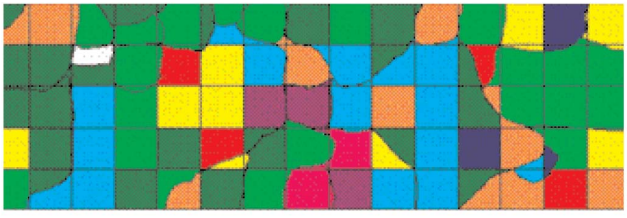

FIG. 3. Strain map for 1-_m-thick Cu sample.

were present, although the exact locations of the boundaries were not determined.

From grain orientation mapping and strain tensor measurements, information was obtained on the distributions of strains for similarly oriented grains and on the grain-to-grain variations of strains. Strain mapping of the perpendicular deviatoric strain ε^*_{33} for the area in Fig. 2 is shown in Fig. 3.

For the Al sample, two thermal cycles were performed at room temperature to 300°C and back to room temperature. Heating and cooling temperatures and times are shown in Fig. 4.

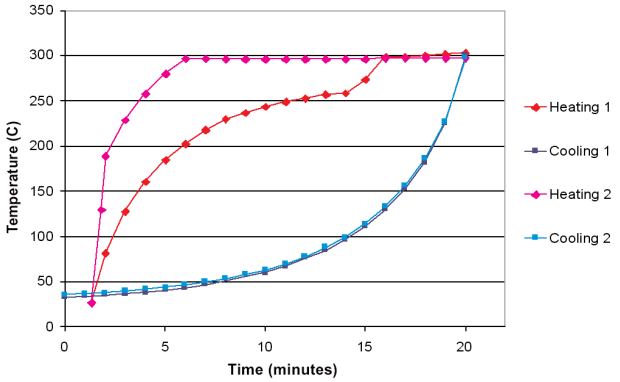

FIG. 4. Temperatures and time for thermal cycles.

Measurements were made at room temperature, during heating, while samples were held at high temperatures, and during cooling. The samples were held at high temperatures for both cycles for 6 h or more, which was long enough for the average strains to relax.

Deviatoric strains were measured during both thermal cycles. Calculations of deviatoric perpendicular strain using differential thermal expansion but without relaxation are shown in Fig. 5, together with experimental data for the two cycles.

In Fig. 5, the experimental data are color-coded to indicate the grain orientations for each data point. No clear trend of different behavior for differently oriented grains is seen.

Thouless et al. [6] proposed deformation mechanism equations for stress development and relaxation in films during thermal cycling that were based on the deformation mechanism maps by Frost and Ashby [7]. Thouless et al. and Vinci et al. [8] used these equations to model thin film behavior during thermal cycling. We also used the equations and material parameters from Frost and Ashby [7] for bulk Al to model our film behavior. The calculated curves are shown in Fig. 6, along with experimental data.

The calculated heating curves for both thermal cycles match experimental data initially when

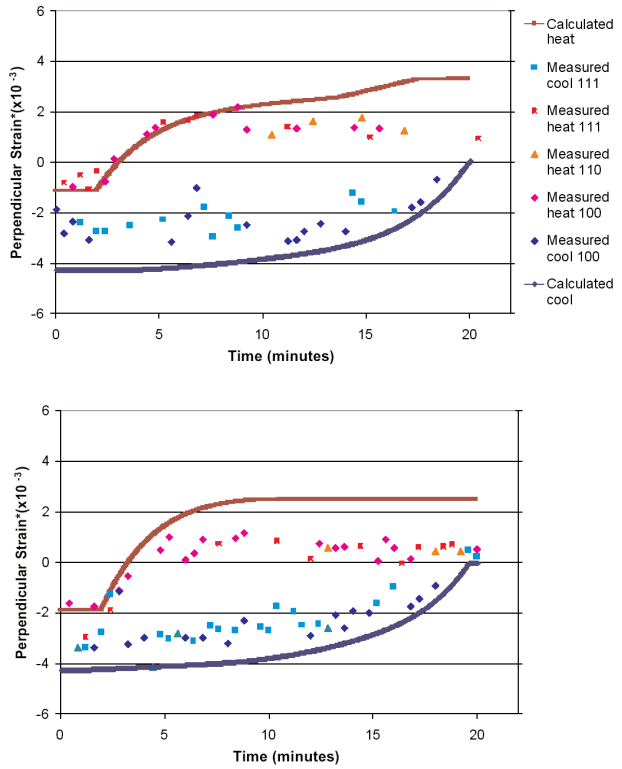

FIG. 5. Perpendicular deviatoric strain versus time for first (top) and second (bottom) thermal cycles for Al sample. Calculated curves do not include relaxation. Differently colored symbols indicate different grain orientations.

relaxation is not included, as shown in Fig. 5. The measured strains are lower than the calculated curves without relaxation after this initial agreement, indicating that relaxation does occur in the sample. The calculated strains including relaxation, shown in Fig. 6, are lower than the experimental data, which indicates that the sample is not relaxing as quickly as the model calculations predict. Calculated cooling curves without relaxation for both thermal cycles show that relaxation occurs in the sample. When relaxation is included in the calculation, there is very little change, probably due to the rapid initial cooling rate.

Grain orientation mapping from area scans taken at room temperature before and after the first thermal cycle are shown in Figs. 7(a) and 7(b). The areas are different due to uncontrolled sample movement during heating and cooling. The hexagon in Fig. 7(c) shows the colors used to represent the different orientations. Black indicates areas that did not index.

Perpendicular deviatoric strain maps for the areas in Figs. 7(a) and 7(b) are shown in Figs. 8(a) and 8(b). Red areas in Fig. 8 are regions of the sample with ε_* of <0, which have higher compressive deviatoric

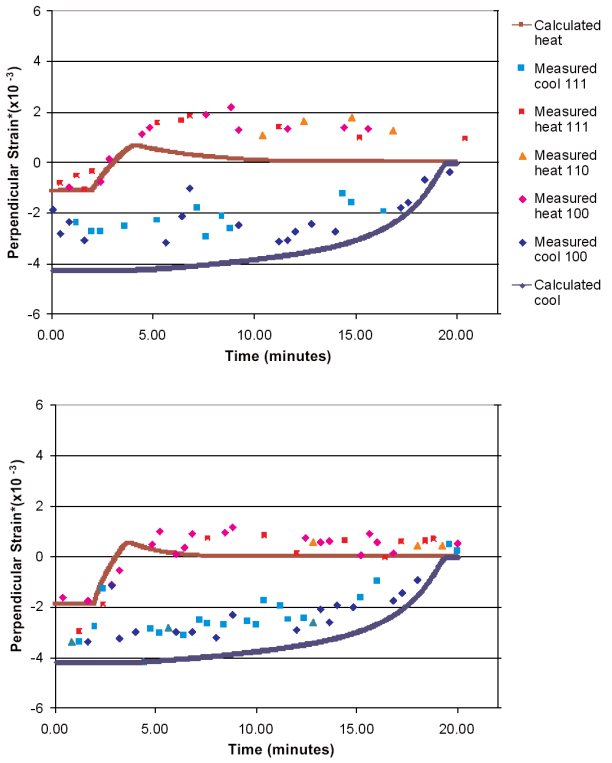

FIG. 6. Perpendicular deviatoric strain versus time for first (top) and second (bottom) thermal cycles for Al sample. Calculated curves include relaxation.

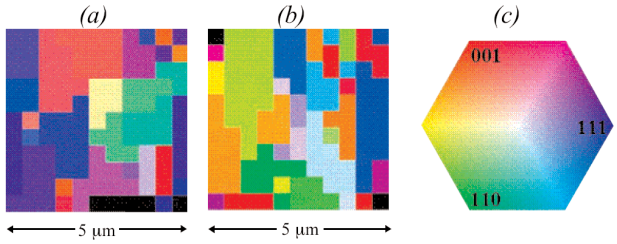

FIG. 7. (a) is an orientation map of Al sample before thermal cycle. (b) is an orientation map of Al sample after thermal cycle. (c) is the orientation legend.

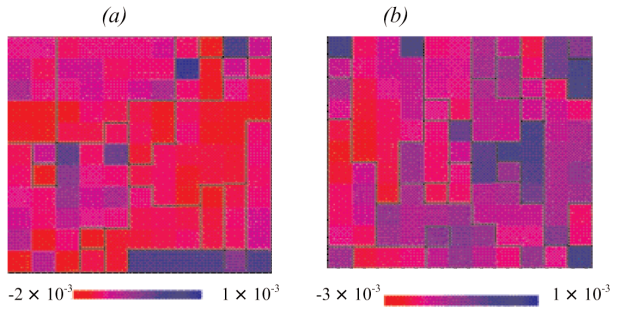

FIG. 8. (a) is a strain map for the area shown in Fig. 7(a). (b) is a strain map for the area shown in Fig. 7(b).

perpendicular strain, as expected, at room temperature. The blue areas are from regions of the sample with $\bar{\varepsilon}^* \approx 0$, or, in some cases $\bar{\varepsilon}^* \geq 0$. A wide range of deviatoric strains exist in the sample. Also, some grains have nearly the same strain throughout their area, while others have large strain gradients from one part of the grain to another.

Discussion

From the Cu orientation and strain maps, it is clear that large strain gradients exist not only in the film in general but within some single grains.

Figs. 5 and 6 show that relaxation is important for the Al sample. However, during heating, the sample is not relaxing as much as this calculation (with bulk material parameters) predicts.

Grain orientation maps and strain maps of the Al sample before and after thermal cycling reveal possible correlations between strain and orientation.

The heating stage is being improved to reduce the amount of thermal drift. *In situ* electromigration-induced strain measurements that use the same heating stage are planned for the near future.

Acknowledgments

This research was supported in part by National Science Foundation (NSF) Grant Nos. DMR-9796284 and DMR-0312189 at Lehigh University and by the SURA/ORNL Summer Cooperative Research Program. ORNL research was sponsored by the U.S. Department of Energy (DOE), Office of Science, Office of Basic Energy Sciences (BES), Division of Materials Sciences, under Contract No. DEAC05-00OR22725 with ORNL managed by UT-Battelle, LLC. Work performed on the UNI-CAT beamline at the APS was supported in part by DOE Grant No. DE-FG02-99ER45743. UNI-CAT is supported by the University of Illinois at Urbana-Champaign, Materials Research Laboratory (DOE; State of Illinois Board of Higher Education, Higher Education Cooperation Act; and NSF); ORNL (DOE under contract with UT-Battelle, LLC); National Institute of Standards and Technology (U.S. Department of Commerce); and UOP LLC. Use of the APS was sponsored by DOE BES under Contract No. W-31-109-ENG-38. We also thank the UNI-CAT staff for support and guidance.

References

[1] J.S. Chung and G.E. Ice, "Automated indexing for texture and strain measurement with broad-bandpass x-ray microbeams," J. Appl. Phys. **86**(9), 5249-5255 (1999).

[2] J.S. Chung, et al., "X-ray microbeam measurement of local texture and strain in metals," Mater. Res. Soc. Symp. Proc. **563**, 169 (1999).

[3] N. Tamura, et al., "High spatial resolution grain orientation and strain mapping in thin films using polychromatic submicron x-ray diffraction," Appl. Phys. Lett., **80**(20), 3724-3726 (2002).

[4] G.S. Cargill, III et al., "X-ray microbeam strain measurements in polycrystalline films," Mater. Sci. Forum **426-432**, 3945-3950 (2003).

[5] L. Moyer, et al., "X-ray microbeam diffraction measurements in polycrystalline aluminum and copper thin films," Mater. Res. Soc. Fall Meeting (to be presented, 2003).

[6] M.D. Thouless, J. Gupta, and J.M.E. Harper, "Stress development and relaxation in copper films during thermal cycling," J. Mater. Res. **8**(8), 1845-1852 (1993).

[7] H.J. Frost and M.F. Ashby, *Deformation-Mechanism Maps: The plasticity and creep of metals and ceramics*, (Pergamon Press, 1982).

[8] R.P. Vinci, E.M. Zielinski, and J.C. Bravman, "Thermal strain and stress in copper thin films," Thin Solid Films **262**, 142-153 (1995).